Synthesized and Characterization TiO2-AlLiH4 Nanostructure for Photocatalytic Activity Application for Removal the Residue of Hydrocarbons in Environment

Moatasem Al Salih[1,*], Riyad E. Abed[2]

[1,*] UPSI university, Faculty of Science and Mathematics, Malaysia

[2]The General Directorate of Education, Thi-Qar Governorate, Iraq.

[2]UPSI university, Faculty of Science, Biology Department.

[1,*]Corresponding Author E-mail: mailto:moatasemalsalih@gmail.com

[2]mailto:riyad.edanabed@nust.edu.iq

Abstract

The novel approach includes The sol-gel technique was used to make titanium dioxide nanoparticles and then for photodegradation Benz[a]anthracene a crystalline, aromatic hydrocarbon, as a trial sample of the residue of hydrocarbons in environments close to oil refining facilities and oil fields, methods, the bandgap was modified by solid-state reaction with Lithium aluminium hydride (AlLiH4) reductive compounds. The optical properties were measured using a UV-visible spectrophotometer (Absorbance (A), energy bandgap (Eg), and absorption coefficient (α). TiO2 and TiO2- solid-state reaction showed a clear blue shift of the absorption bandgap which were (2.8ev, 2.7ev, 2.25ev, 2.0ev) to) TiO2, calcination TiO2-AlLiH4 (500C°) then TiO2 -AlLiH4 (750 C°)) respectively. The structure of prepared TiO2 Nanopowders was identified using XRD, Distribution of particle size varied significantly compared to the Sheerer formulation predicted crystallite size (D). which was in a good accordant compared with ASTM results, the particle size and their distribution were characterized using (AFM). To the surface forms and compositions diameters of nanoparticles) SEM) was implemented. The microanalysis of energy scattering X-ray (EDX) was used to examine the chemical makeup of the entire samples. Using UV-Vis spectrophotometry, the photocatalytic response was examined. The photocatalyst impact on the benz[a]anthracene decomposition rate by using catalyst TiO2- and solid-state (TiO2-NaBH4 (550,750)) and (TiO2-AlLiH4 (500,750 C°). A photocatalytic effect is the

catalyst's influence on the catalyst. Using the constant weight of the catalyst and benz[a]anthracene The most effective weight was found (1*10-4 M).

Keywords: Nanocomposite, Hydrocarbons removal, Photocatalytic, TiO_2 - AlLiH4.

<div dir="rtl">

الخلاصة:

يتضمن النهج الجديد استخدام تقنية sol-gel لتصنيع جسيمات نانوية لثاني أكسيد التيتانيوم لاجل التحلل الضوئي أنثراسين بنز اي والذي يعد هيدروكربون بلوري عطري، كعينة تجريبية لبقايا الهيدروكربونات في بيئات قريبة من منشآت تكرير النفط وحقول النفط. تم تعديل فجوة الحزمة عن طريق تفاعل الحالة الصلبة مع مركبات اختزال هيدريد الألومنيوم الليثيوم. تم قياس الخواص الضوئية باستخدام مقياس طيف ضوئي مرئي للأشعة فوق البنفسجية الامتصاصية ، و قياس فجوة الطاقة (على سبيل المثال)، ومعامل الامتصاص أظهر تفاعل TiO2 و TiO2-الحالة الصلبة انزياحًا أزرقًا واضحًا لفجوة الامتصاص التي كانت ٢،٨ ـ ٢،٧-٢،٢٥-٢،٠٠ الكترون فولت عند درجة كلسنة ٥٠٠ درجة مئوية ثم رفعها إلى ٧٥٠ درجة مئوية على التوالي. تم التعرف على بنية مساحيق TiO2 النانوية المحضرة باستخدام XRD ، حيث اختلف توزيع حجم الجسيمات بشكل كبير مقارنة بالصيغة المتنبأ بها بالحجم البلوري والتي كانت في توافق جيد مقارنة بنتائج ASTM ، وتم تمييز حجم الجسيمات وتوزيعها باستخدام (AFM) تم دراسة الأشكال والتركيبات السطحية بأقطار الجسيمات النانوية (SEM). تم استخدام التحليل المجهري للأشعة السينية المشتتة للطاقة (EDX) لفحص التركيب الكيميائي للعينات بأكملها. باستخدام القياس الطيفي بالأشعة المرئية وفوق البنفسجية ، تم فحص استجابة التحفيز الضوئي. تأثير المحفز الضوئي على انثراسين البنزين [أ] لملاحظة معدل تحلل الأنثراسين باستخدام المحفز TiO2- الحالة الصلبة (TiO2-NaBH4 (550.750)) و TiO2-AlLiH4 (500.750) درجة مئوية). التأثير التحفيزي هو تأثير المحفز على المحفز باستخدام الوزن الثابت للعامل المحفز والبنز [أ] أنثراسين تم العثور على الوزن الأكثر فعالية (1 * 10-4 م).

</div>

1. Introduction

Anion doping in broad band gap photo catalysts active under UV irradiation is another way to improve the visible light response [1-3]. Development of visible light photo catalysts from oxide semiconductors by doping with anions as examples (C, N, F, P, and S). The sol-gel technique was used to make AlLiH4-doped TiO2, with different titania precursors and nitrogen sources. Utilizing titanium(IV) tetraisopropoxide with AlLiH4solution and calcined at 673 K, it was discovered that AlLiH4-doped TiO2 using titanium(IV) tetraisopropoxide with AlLiH4solution offered the most suitable characteristics for serving as the photo catalyst [5-8]. The TGA, Raman, and XRD findings showed that this AlLiH4-doped TiO2 catalyst had a high crystallinity since the titania precursor had been fully hydrolyzed, with no organic component to obstruct initial phase formation. The results of SEM and TEM showed that the surface shape

was spherical, similar to fluffy powders [8-11]. Furthermore, the inserted metal or non-metals that's slowed the anatase-to-rutile phase transition as the calcination temperature rose. The findings of the elemental analysis and UV-Vis/DR showed that ions, metals, and nonmetals may be latent in the TiO2 lattice with strong connections, producing an influence on the band gap structure by adding energy levels near the valence band of TiO2. Under visible light, all of these characteristics improved the photocatalytic activity of co-doped TiO2 [12-15]. In terms of photocatalytic activity, TiO2 - AlLiH4 calcined at 673 K with titanium(IV) tetraisopropoxide and ammonia solution degraded phenanthrene, benz[a]anthracene, and phenol with the best efficiency. When calcined at a higher temperature, however, its photocatalytic activity was substantially reduced. In the instance of photodegradation of phenanthrene, a plausible mechanism was postulated based on two GC/MS identified intermediates: bis(2-ethylhexyl) benzene-1,2-dicarboxylate and dimethyl-4-methyl-1,2-benzene dicarboxylate.[13-22] Incomplete combustion of organic matter produces benz[a]anthracene, a crystalline aromatic hydrocarbon with four fused benzene rings. Benz(a)anthracene can be found in gasoline and diesel exhaust, tobacco and cigarette smoke, coal tar and coal tar pitch, coal combustion emissions, charcoal-broiled foods, amino acids, fatty acids, and carbohydrate pyrolysis products, wood and soot smoke, and creosote, asphalt, and mineral oils, among other things. Only for research purposes is this chemical utilized. It's safe to assume that benz(a)anthracene is a human carcinogen. [23-27] (NCI05).
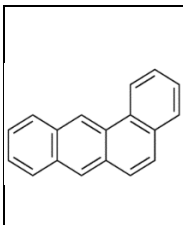
1.1 NCI Thesaurus (NCIt)

Colorless leaflets or plates, as well as coarse gold powder with a greenish-yellow fluorescence, are found in benz[a]anthracene. It's possible that this substance is carcinogenic. [15, 28]

1.2 CAMEO Chemicals

Tetraphene is a four-fused benzene ring polycyclic arene with an angular ortho-fused structure. It is a tetraphenes member and an ortho-fused polycyclic arene. First and foremost, phenanthrene is a PAH made up of three fused benzene rings (Table 1). It is a recognized irritant that photosensitizes skin to light and is present in cigarette smoke.

Phenanthrene is a white powder that is soluble in most organic solvents but insoluble in water. Second, benz[a]anthracene is a PAH [28-30], that has a four-member ring structure, as illustrated in Table (1). It is a natural substance that is created when organic material is incompletely burned. The toxicity of benz[a]anthracene and other PAHs is largely focused at tissues with growing cells [31-33]. Some TiO_2 - $AlLiH_4$ will be used in the photocatalytic degradation of benz[a]anthracene. Also investigated were the photocatalytic activity and rate constants of each TiO_2 - $AlLiH_4$ and P25 TiO_2.

Table (1) The structures and general properties of phenanthrene and benz[a]anthracene.[33]

Structure	Properties			
	Molecular formula	Molecular weight (g/mol)	Melting point (K)	Boiling point (K)
	$C_{18}H_{12}$	228.29	158	438

Authores prepare and calcined TiO_2 - $AlLiH_4$ at 593 K using a modified sol-gel hydrothermal process using tetrabutyl titanate as the precursor [34]. XRD research provided strong evidence for TiO_2's heterogeneous crystal lattice structure. The particle size distribution was narrow, with an average particle size of 13.5 nm. The high visible-light absorption of $AlLiH_4$-doped TiO_2 was apparent in UV-Vis spectra, which extended beyond 550 nm. The as-prepared sample included Ti-O, N-H, TiO-H, H-O-H, and Ti-NOx groups, and the formation of –Ti-NOx (-Ti-O-N-Ti-) might suggest that N atoms were integrated into the TiO2 crystal lattice, which was compatible with XPS data. The thermal study showed that AlLiH4doped TiO2 may inhibit the phase change of anatase to rutile, because most TiO2 particles were converted into rutile at 973 K in pure TiO2. From all of these characteristics, the AlLiH4-doped TiO2 (A/R = 4:1) mixed crystal sample had strong visible-light response photocatalytic activity, which was

attributed to a synergistic impact among its surface acidity, surface chemistry, and surface doping AlLiH4 atoms in mixed crystals has a chemical impact. The adsorption of cationic organic molecules was increased when the acidic surface was reduced. The doping co atoms increased visible-light absorption, and the mixed crystal effect might have a number of positive impacts on photocatalytic activity.

utilized a titanium(IV) (diisopropoxide)bis(2,4-pentadionate) precursor and various nitrogen and sulfur sources to create N- and/or S-doped TiO2 in a sol-gel process. According to the TGA-DTA statistics, the weight reduction was between 40 and 60 percent. The main homogeneous crystalline phase in the N- and/or S-doped TiO2 samples was anatase, as shown by XRD patterns. The process of absorption [35].

The profile of AlLiH$_4$doped TiO$_2$ moved into visible areas (400-500 nm) when compared to P25 TiO$_2$, owing to band gap narrowing of doped TiO2. Under visible light, the effect of N and/or S doping increased the photocatalytic activity of titania powders as measured by Congo red dye discoloration. Because the crystallinity of anatase was enhanced by S-doping, S-doped TiO$_2$ had the greatest activity among the doped TiO$_2$. Furthermore, sulfur atoms inhibited the anatase to rutile phase transition. Palgrave et al. (2008) used high-resolution XPS to investigate the electrical structure of co-doped TiO$_2$, which was made by annealing single crystal rutile (110) substrates in NH3 at high temperatures [38]. The results indicated that ammonia treatment at 873 K resulted in the integration of AlLiH$_4$ ^{2}p states at the valence band's top without a decrease of Ti4+ to Ti3+. The introduction of AlLiH$_4$ ^{2}p states happened at the same location after annealing at 973 K, but it resulted in surface decrease. The band gap in the valence region photoemission spectra narrowed as a result of the doping.

Aimed to study the photochemical reaction of benz[a]anthracene on TiO$_2$ particles [36]. The rising in situ DRIFTS peaks at wavenumbers of 2697 and 3762 cm-1, which correspond to surface hydroxyl properties, led them to the conclusion that this reaction took place on the surface of TiO$_2$ particles. Furthermore, a wide band centered at 3608 cm-1 and a band at 1620 cm-1 diminished with time, indicating that adsorbed H2O dissolved to produce hydroxyl. The major photoproduct was identified as benz[a]anthracene-7,12-dione based on GC/MS findings [37].

2. <u>Methods</u>

Using titanium tetraisopropoxide and a Sol-Gel technique, nano-TiO_2 powder was created (TTIP), according to the [15, 16-39].

2.1 Solid State Reaction of TiO_2

Different weights of powder TiO_2 were mixed with equal proportions of NaBH4 and repeated for $AlLiH_4$. Then, calcination process at different temperatures in the furnace to produce in hydrogen gas by dissociation AlLiH4 and NaBH4 at varies temperatures 500 and 550 according to convert TiO_2 by reduction process from anatase to rutile at 600 and 800. The calcination continues for 2h, were the powder appear in black and white colors according to calcination temperature. Then, the ratio (1:1) products (TiO2:NaBH$_4$) and (TiO2:AlLiH$_4$) have been characterization by X-ray diffraction, SEM, EDX, AFM and solid state UV-VIS spectrometer.

2.2 Preparation of benz[a]anthracene solution

25.00 ml of 1000 ppm stock benz[a]anthracene solution in pure methanol solvent was prepared by dissolving 0.0250 g standard benz[a]anthracene with a certain volume in a 25 ml volumetric flask. 500.00 ml of 20 ppm benz[a]anthracene solution was prepared by diluting 10.00 ml of stock benz[a]anthracene solution with distilled water and methanol in the volumetric ratio of 1:3. Concurrently, benz[a]anthracene solution was also sonicated, [40-41]

2.3The calibration curve of benz[a]anthracene solution

Initially, the series of benz[a]anthracene concentrations, 1, 2, 3, 4 and 5 ppm, were prepared by diluting from 20 ppm of benz[a]anthracene solution (as prepared in section 5.2) with the volume of 0.50, 1.00, 1.50, 2.00 and 2.50 ml, respectively. After that, diluted solution was made up the volume to 10 ml by distilled water and, finally, it was ready to measure fluorescence emission using a Perkin Elmer Lambda 35 luminescence spectrophotometer. [39-41]

2.4 Photo degradation of benz[a]anthracene

Five hours consisting of one hour in dark reaction and four hours in photoreaction were set up for benz[a]anthracene degradation. Under the photoreaction, the sample was collected every 30 min until 90 min of degradation. After that, the sample was continually collected every hour. All of samples were taken by passing the general process as mentioned above. Then, only 1 ml of a sample was picked up using an autopipette from the centrifuged sample and made up the volume by distilled water in a 10 ml volumetric flask. Fluorescent measurement at λ_{em} of 527 nm was applied to detect the concentration of each sample. All samples were also conducted in three replicates. [19, 33, 35, 40]

2.5 Luminescence Spectrophotometry

The decreasing concentration of reactants namely benz[a]anthracene was followed by measuring the absorption on a Perkin Elmer Lambda 35 spectrophotometer. To get an obvious spectrum, emission slit width or excitation slit width should be also adjusted to find the appropriate condition. Eventually, for benz[a]anthracene, the optimized condition was λ_{ex} at 287.0 nm, with a scan speed of 1000 nm/min, the excitation slit width is 10.0 nm and the emission slit width is 2.5 nm [5,13,33].

3. <u>Result and Discussion</u>

3.1 Photo degradation of benz[a]anthracene

This section made only use of $AlLiH_4$-doped TiO_2 using titanium(IV) tetraisopropoxide mixed with $AlLiH_4$ and calcined at 673 K as a photocatalyst due to its most appropriate photocatalytic properties such as crystallinity, phase composition, surface morphology as well as $AlLiH_4$ quantity.
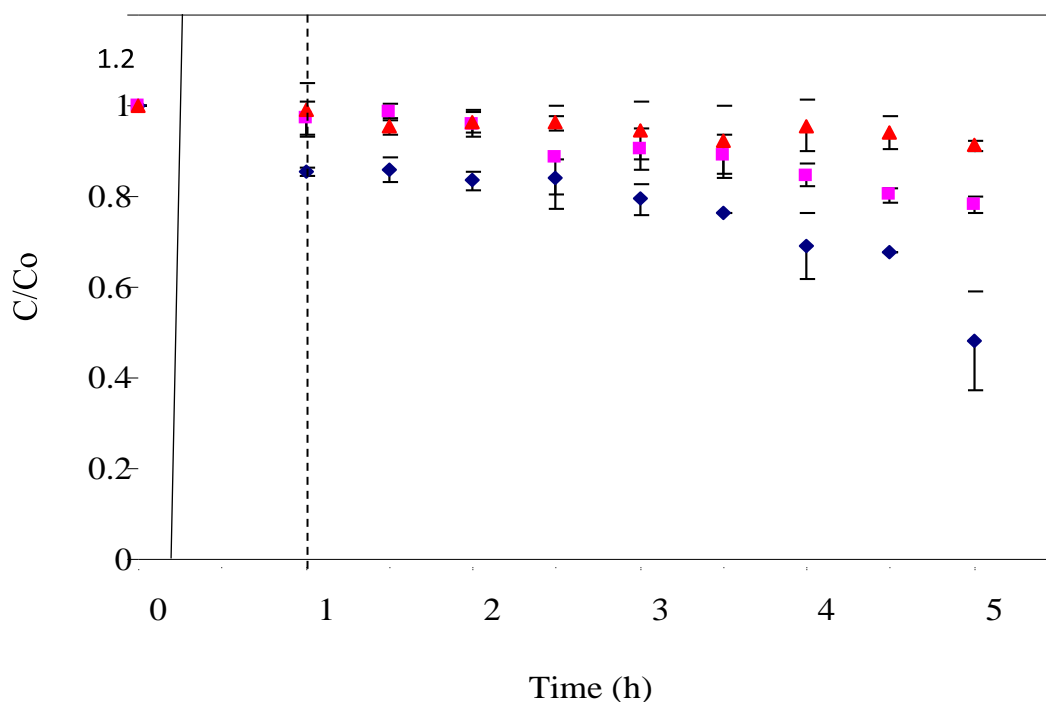
Fig. (1): Photo degradation of benz[a]anthracene by using; (a) AlLiH₄ doped TiO₂ calcined at 673 K (♦), (b) P25 TiO₂ (■) and (c) without catalysts (▲).

The result as shown in Figure (1) suggests that $AlLiH_4$-doped TiO_2 could catalyze the photo degradation reaction of benz[a]anthracene with 52% conversion. It degraded with the rate constant of 0.074 h^{-1} as shown in Table (2). In spite of no results about detected intermediate products, it is assured that the reduction of relative concentration of benz[a]anthracene originated from the $AlLiH_4$-doped TiO_2 effect. Because, in case of no catalyst, there was simply 8% conversion of benz[a]anthracene this results correspondence with [19, 33, 37,40-43] $AlLiH_4$-doped TiO_2 prepared with the variation of titania precursors and $AlLiH_4$ sources was able to be synthesized by the sol-gel method. From all characterization techniques, it can be implied that the calcination temperature had a significant impact on the crystal structure of $AlLiH_4$-doped TiO_2. With the increasing temperature, $AlLiH_4$-doped TiO_2 got the larger crystallite size, the higher crystallinity and Transformation of anatase-to-use phase. The lowest crystallite size, the greatest anatasis and the high number of firmly bound Nitrogen are optimal for the best photocatalytic activity under visible light for AlLiH4-doped TiO_2.

Titanium (IV) Tetraisopropoxide as a titanium precursor combined to NH3 as a nitrogen source is calcined to 674 K compared to all AlLiH$_4$-doped-TiO$_2$, and AlLiH4-doped-TiO$_2$ seemed to be closely within the scope of the ideal photo catalyst. It provided high crystallinity and spherical surface morphology although its crystallite size is 16 nm. Its phase transformation was retarded by the effect of the strongly-bonded nitrogen in TiO$_2$ lattice. Moreover, the structural determination did also support that the structure of Titanium (IV) tetraisopropoxide was easy to be hydrolyzed by ammonia or water molecules. With regard to photocatalytic activity, AlLiH$_4$-doped TiO$_2$ using titanium(IV) tetraisopropoxide mixed with NH$_3$ and calcined at 673 K provided the highest %conversion among three substrates; 33% of 20 ppm phenanthrene, 52% of 20 ppm benz[a]anthracene and 4% of 20 ppm phenol. It also rendered the fastest rate of reactions, which was able to be observed from the rate constants; 0.058 h^{-1} for phenanthrene, 0.074 h^{-1} for benz[a]anthracene, and 0.036 h^{-1} for phenol. Interestingly, the elevating temperature had an adverse repercussion on photocatalytic activity.

which resulted from thermal decomposition. Meanwhile, P25 TiO2 has a good ability to degrade benz[a]anthracene up to 22% conversion with the rate constant of 0.058 h-1 because of synergistic effect between anatase and rutile, like photodegradation of phenanthrene.

Table (2) %Conversion and rate constants of photodegradation reactions of three substrates by N-doped TiO2 using Titanium(IV) Tetraisopropoxide mixed with NH3 and calcined at 673 K.

Photocatalyst	Phenanthrene			Benz[a]anthracene			Phenol		
	% Conversion[a]	R^2	Rate constant[b] (h^{-1})	% Conversion	R^2	Rate Constant (h^{-1})	% Conversion	R^2	Rate Constant (h^{-1})
AlLiH4-doped	33	0.9991	0.058	52	0.9215	0.074	4	0.9185	0.0036
P25 TiO$_2$	12	0.8093	0.052	22	0.9227	0.058	2	0.8737	0.0026

[a]% The conversion has been determined from ($I_{nitial} - C_{final}$ / I_{nitial}) x100%.

[b]e a procedure to calculate rate constants are also shown in Appendix

In addition, the probable mechanism of the photodegradation reaction of phenanthrene was proposed based on the two detectable intermediates. A series of dark reactions with absorbance measurement by UV-Vis spectrophotometry, within different periods with the change of pH and temperature. The results indicate that no degradation of the methylene blue dye although all the factors affecting photocatalytic present except UV-light. At the best weight, the influence of many factors on The organic pollutants decomposition rate was investigated, with pH changes varying from acid to non-neutral and alkaline in acid conditions (4.5, 7.1, and 9.4) as the greatest percentage in benz[a]anthracene breakdown. The effects of change in temperature from (20, 30, 40°C) showed that the breakdown rate increased as the temperature for the MB rose. Energy activation (Ea) has equations as follows: where: k: first-order rate constant (min-1) C0: initial concentration Ct: concentration after time . The rate constant for degradation benz[a]anthracene was calculated from a graph Figure (2 a,b) which is a linear plot between (In (Ct/C0) versus (t). From slope = -k which equals (-k) according to the equation above are listed and Table (2).

The results in Figure (2) show the increase in temperature (293-313) K will increases the discoloration rate of benz[a]anthracene, and also the rate constant increase explained by the fact adsorption is an endothermic process.

been calculated for respective response by expending the equation of Arrhenius equation between (5.73–11.31) kJ mol⁻
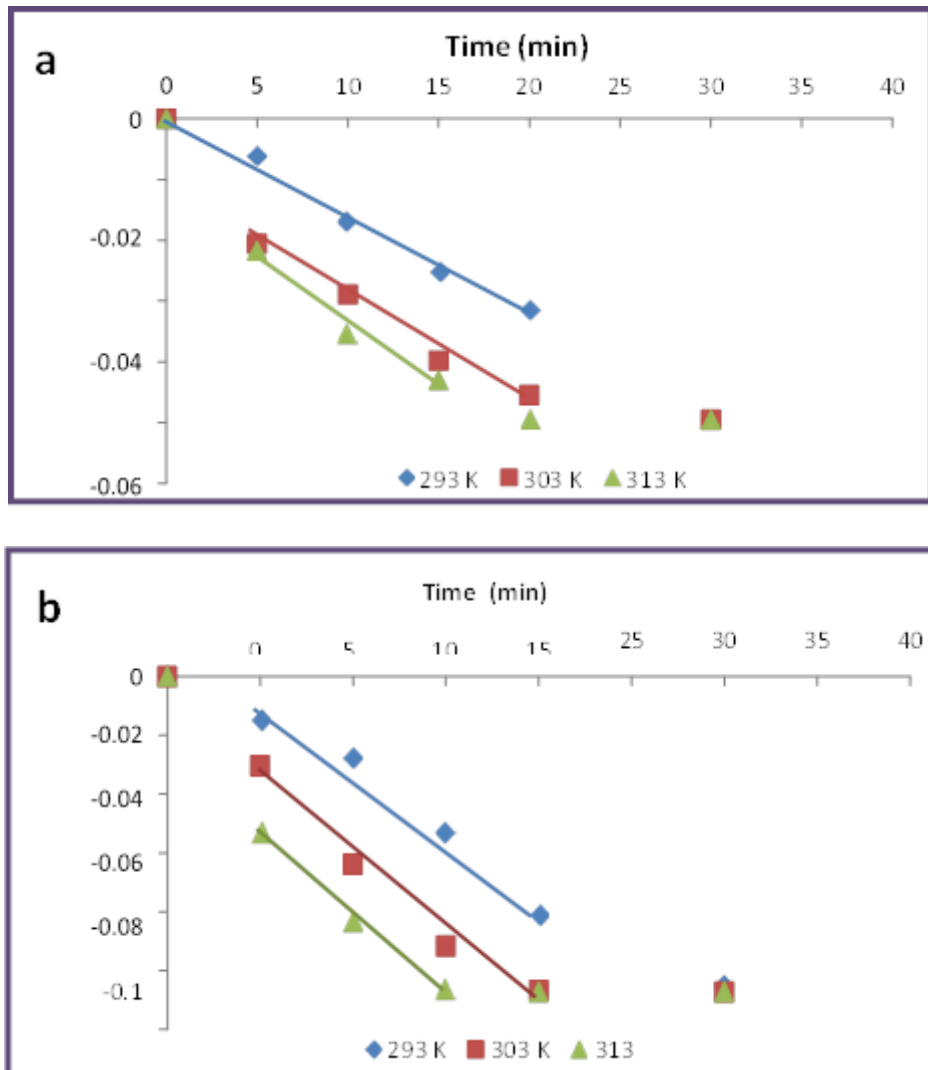
Fig. (2): Plot of time versus. ln (C/C0) using a TiO$_2$ -AlLiH4
a- TiO$_2$ -AlLiH$_4$ (500) b- TiO$_2$ -AlLiH4 (750)

It was found that the benz[a]anthracene decolorization was obeyed the first-order rate law. Because interactions depend only on the degradation of benz[a]anthracene to it that the highest concentration which is considered basic material interaction, which can be expressed by Kinetic of Degradation of benz[a]anthracene.

4. <u>Conclusion</u>

TiO2-AlLiH4 prepared with the variation of titania precursors and AlLiH4 sources were able to be synthesized by the sol-gel method. From all characterization techniques, it can be implied that the calcination temperature had a significant impact on the crystal structure of TiO2-AlLiH4. With the increasing temperature, TiO2-AlLiH4 got the larger crystallite size, the higher crystallinity, and anatase-to-rutile phase transformation. The smallest crystallite size, the highest anatase crystallinity, and a large amount of strongly-bonded AlLiH4 are the ideal properties of AlLiH4-doped TiO2 for the maximum photocatalytic activity under visible light. Compared to all TiO2-AlLiH4, calcined at 750 K seemed to be closed within the scope of the ideal photocatalyst. It provided high crystallinity and spherical surface morphology although its crystallite size is 16 nm. Concerning photocatalytic activity, TiO_2-$AlLiH_4$ using calcined at (500,750 C°). Provided the highest rate conversion among three substrates; 52% of 20 ppm benz[a]anthracene and 4% of 20 ppm phenol. It also rendered the fastest rate of reactions, which was able to be observed from the rate constants; 0.058 h-1 for phenanthrene, 0.074 h-1 for benz[a]anthracene, and 0.036 h-1 for phenol. Interestingly, the elevating temperature had an adverse repercussion on photocatalytic activity. In addition, the probable mechanism of the photodegradation reaction of phenanthrene was proposed based on the two detectable intermediates.

References

[1] Patil SB, Basavarajappa PS, Ganganagappa N, Jyothi MS, Raghu AV, Reddy KR. Recent advances in non-metals-doped TiO2 nanostructured photocatalysts for visible-light-driven hydrogen production, CO2 reduction, and air purification. International Journal of Hydrogen Energy. 2019 May 21; 44(26):13022-39.

[2] Etacheri V, Di Valentin C, Schneider J, Bahnemann D, Pillai SC. Visible-light activation of TiO2 photocatalysts: Advances in theory and experiments. Journal of Photochemistry and Photobiology C: Photochemistry Reviews. 2015 Dec 1;25:1-29.

[3] Pelaez M, Nolan NT, Pillai SC, Seery MK, Falaras P, Kontos AG, Dunlop PS, Hamilton JW, Byrne JA, O'Shea K, Entezari MH. A review on the visible light active titanium dioxide photocatalysts for environmental applications. Applied Catalysis B: Environmental. 2012 Aug 21;125:331-49.

 [4] Yunus, N. N., F. Hamzah, M. S. So'Aib, and J. Krishnan. "Effect of catalyst loading on photocatalytic degradation of phenol by using N, S Co-doped TiO2." In IOP Conference Series: Materials Science and Engineering, vol. 206, no. 1, p. 012092. IOP Publishing, 2017.

[5] Rajalakshmi K. Photocatalytic Reduction of Carbon dioxide in conjunction with the decomposition of water on oxide semiconductor surfaces. Indian Institute of Technology, Madras, India. 2011.

[6] Zaker, Y., Hossain MA, M. Ali, M. S. Islam, and T. S. A. Islam. "Characterization of sand fractionated from Bijoypur soil, Bangladesh and its application as an adsorbent." Research Journal of Chemical Sciences ISSN 2231 (2013): 606X.

[7] Liu, Jincheng, Hongwei Bai, Yinjie Wang, Zhaoyang Liu, Xiwang Zhang, and Darren Delai Sun. "Self-assembling TiO2 nanorods on large graphene oxide sheets at a two-phase interface and their anti-recombination in photocatalytic applications." Advanced Functional Materials 20, no. 23 (2010): 4175-4181.

[8] AlSalih, Moatasem, Syakirah Samsudin, and Siti Suri Arshad. "Synthesis, Properties and Application of Titanium Dioxide Doped with Nitrogen. Its Effectiveness on Photo Degradation Glutathione-S-Transferase (GST) enzymes Pupae Instar of Aedes aegypti." In Journal of Physics: Conference Series, vol. 1963, no. 1, p. 012131. IOP Publishing, 2021.

[9] Ong, Wee-Jun, Lling-Lling Tan, Siang-Piao Chai, Siek-Ting Yong, and Abdul Rahman Mohamed. "Highly reactive {001} facets of TiO 2-based composites: synthesis, formation mechanism and characterization." Nanoscale 6, no. 4 (2014): 1946-2008.

[10] Sudha, D., and P. Sivakumar. "Review on the photocatalytic activity of various composite catalysts." Chemical Engineering and Processing: Process Intensification 97 (2015): 112-133.

[11] Zhang, Wei, Yong Tian, Haili He, Li Xu, Wei Li, and Dongyuan Zhao. "Recent advances in the synthesis of hierarchically mesoporous TiO2 materials for energy and environmental applications." National Science Review 7, no. 11 (2020): 1702-1725.

[12] Al-Mamun, M. R., S. Kader, M. S. Islam, and M. Z. H. Khan. "Photocatalytic activity improvement and application of UV-TiO2 photocatalysis in textile wastewater treatment: A review." Journal of Environmental Chemical Engineering 7, no. 5 (2019): 103248..

[13] Hao, Dandan, Yudi Yang, Bi Xu, and Zaisheng Cai. "Bifunctional fabric with photothermal effect and photocatalysis for highly efficient clean water generation." ACS Sustainable Chemistry & Engineering 6, no. 8 (2018): 10789-10797.

[14] Yang, Jinhui, and Xiaogang Luo. "Ag-doped TiO2 immobilized cellulose-derived carbon beads: One-Pot preparation, photocatalytic degradation performance and mechanism of ceftriaxone sodium." Applied Surface Science 542 (2021): 148724.

[15] Lee, Sang-Hwan, Won-Seok Lee, Chang-Ho Lee, and Jeong-Gyu Kim. "Degradation of phenanthrene and pyrene in rhizosphere of grasses and legumes." Journal of Hazardous Materials 153, no. 1-2 (2008): 892-898.

[19] Rani, Manviri, and Uma Shanker. "Sunlight mediated improved photocatalytic degradation of carcinogenic benz [a] anthracene and benzo [a] pyrene by zinc oxide encapsulated hexacyanoferrate nanocomposite." Journal of Photochemistry and Photobiology A: Chemistry 381 (2019): 111861.

[20] Guo, Jin, Xiuchu Liu, Xiaomei Zhang, Juan Wu, Chao Chai, Dong Ma, Qinghua Chen, Dan Xiang, and Wei Ge. "Immobilized lignin peroxidase on Fe3O4@ SiO2@ polydopamine nanoparticles for degradation of organic pollutants." International journal of biological macromolecules 138 (2019): 433-440.

[21] Bagheri, Samira, Zul Adlan Mohd Hir, Amin Termeh Yousefi, and Sharifah Bee Abdul Hamid. "Progress on mesoporous titanium dioxide: synthesis, modification and applications." Microporous and Mesoporous Materials 218 (2015): 206-222.

[22] Deng Y, Wei J, Sun Z, Zhao D. Large-pore ordered mesoporous materials templated from non-Pluronic amphiphilic block copolymers. Chemical Society Reviews. 2013, 42(9):4054-70.

[23] Kim, Ki-Hyun, Shamin Ara Jahan, Ehsanul Kabir, and Richard JC Brown. "A review of airborne polycyclic aromatic hydrocarbons (PAHs) and their human health effects." Environment international 60 (2013): 71-80. [24] WRITER HA. LEVELS OF POLYCYCLIC AROMATIC HYDROCARBON IN FRESHWATER FISH DRIED UNDER DIFFERENT DRYING REGIMES. 2021

[25] Giri SK, Kumar A, Kumar A, Gulati S. Effects of Polycyclic Aromatic Hydrocarbons on Environment Health. ICRIET-2016; ISBN: 978-93-856181-6

[26] Alegbeleye, Oluwadara Oluwaseun, Beatrice Oluwatoyin Opeolu, and Vanessa Angela Jackson. "Polycyclic aromatic hydrocarbons: a critical review of environmental occurrence and bioremediation." Environmental management 60, no. 4 (2017): 758-783.

[27] Rabani, Mir Sajad, Aukib Habib, and Mahendra Kumar Gupta. "Polycyclic Aromatic Hydrocarbons: Toxic Effects and Their Bioremediation Strategies." In Bioremediation and Biotechnology, Vol 4, pp. 65-105. Springer, Cham, 2020.

[28] Bäumler, Wolfgang. "Chemical hazard of tattoo colorants." La Presse Médicale 49, no. 4 (2020): 104046.

[29] Neff, Jerry M., Scott A. Stout, and Donald G. Gunster. "Ecological risk assessment of polycyclic aromatic hydrocarbons in sediments: identifying sources and ecological hazard." Integrated Environmental Assessment and Management: An International Journal 1, no. 1 (2005): 22-33.

[30] Hartwig, Andrea, ed. The MAK-Collection for Occupational Health and Safety: Part I: MAK Value Documentations, Volume 27. John Wiley & Sons, 2013.

[31] Idowu, Oluyoye, Kirk T. Semple, Kavitha Ramadass, Wayne O'Connor, Phil Hansbro, and Palanisami Thavamani. "Beyond the obvious: Environmental health implications of polar polycyclic aromatic hydrocarbons." Environment international 123 (2019): 543-557.

[32] Goldizen, Fiona C., Peter D. Sly, and Luke D. Knibbs. "Respiratory effects of air pollution on children." Pediatric pulmonology 51, no. 1 (2016): 94-108.

[33] Mackie, Cameron J., Tao Chen, Alessandra Candian, Timothy J. Lee, and Alexander GGM Tielens. "Fully anharmonic infrared cascade spectra of polycyclic aromatic hydrocarbons." The Journal of chemical physics 149, no. 13 (2018): 134302.

[34] Huang, Jianshe, Yang Liu, Haoqing Hou, and Tianyan You. "Simultaneous electrochemical determination of dopamine, uric acid and ascorbic acid using palladium nanoparticle-loaded carbon nanofibers modified electrode." Biosensors and Bioelectronics 24, no. 4 (2008): 632-637.

[[35] Ksibi, Mohamed, Sylvie Rossignol, Jean-Michel Tatibouët, and Christos Trapalis. "Synthesis and solid characterization of nitrogen and sulfur-doped TiO2 photocatalysts active under near visible light." Materials Letters 62, no. 26 (2008): 4204-4206.

[36] Chen, Ying-Li, and Qian-Zhong Li. "Prediction of apoptosis protein subcellular location using improved hybrid approach and pseudo-amino acid composition." Journal of theoretical biology 248, no. 2 (2007): 377-381.

[37] Shen, Jiandong, Shicheng Zhang, Jinjun Lian, Lingdong Kong, and Jianmin Chen. "Benz [a] anthracene heterogeneous photochemical reaction on the surface of TiO2 particles." Acta Physico-Chimica Sinica 23, no. 10 (2007): 1531-1536.

[38] Boscher, Nicolas D., Claire J. Carmalt, Robert G. Palgrave, and Ivan P. Parkin. "Atmospheric pressure chemical vapour deposition of SnSe and SnSe2 thin films on glass." Thin solid films 516, no. 15 (2008): 4750-4757.

[39] Qiu, Shipeng, and Samar J. Kalita. "Synthesis, processing and characterization of nanocrystalline titanium dioxide." Materials Science and Engineering: A 435 (2006): 327-332.

[40] Odum, Jay R., Stephen R. McDow, and Richard M. Kamens. "Mechanistic and kinetic studies of the photodegradation of benz [a] anthracene in the presence of methoxyphenols." Environmental science & technology 28, no. 7 (1994): 1285-1290.

[41] AlSalih Et Al, Moatasem. "Adjustment and Application of the Band Gap of Nano Titanium Dioxide: Its Usefulness on Photo degradation of Wastewater (phenol)." Egyptian Journal of Aquatic Biology and Fisheries 25, no. 3 (2021): 815-830.

[42] Sims, P. "Epoxy derivatives of aromatic polycyclic hydrocarbons. The preparation of benz [a] anthracene 8, 9-oxide and 10, 11-dihydrobenz [a] anthracene 8, 9-oxide and their metabolism by rat liver preparations." Biochemical Journal 125, no. 1 (1971): 159-168.

[43] Al Salih, Seenaa Wdaah, Moatasem Al Salih, and Syakirah Samsudin. "MODIFICATION OF THE BAND GAP OF NANO TITANIUM DIOXIDE, ITS APPLICATION AND EFFECTIVENESS ON PHOTO DEGRADATION OF ORGANIC POLLUTANTS.